

# Germ Cell Survival Through Carbohydrate-Mediated Interaction with Sertoli Cells

Tomoya O. Akama,<sup>1</sup> Hiroaki Nakagawa,<sup>1,3</sup> Kazuhiro Sugihara,<sup>1,4</sup> Sonoko Narisawa,<sup>2</sup> Chikara Ohyama,<sup>5</sup> Shin-Ichiro Nishimura,<sup>3</sup> Deborah A. O'Brien,<sup>6</sup> Kelley W. Moremen,<sup>7</sup> José Luis Millán,<sup>2</sup> Michiko N. Fukuda<sup>1\*</sup>

Spermatogenesis is a precisely regulated process in which the germ cells closely interact with Sertoli cells. The molecular basis of this cell-cell adhesion is unknown. Here, we demonstrate that targeted disruption of *Man2a2*, a gene encoding  $\alpha$ -mannosidase IIx (MX), an enzyme that forms intermediate asparagine-linked carbohydrates (*N*-glycans), results in *Man2a2* null males that are largely infertile. The *Man2a2* null spermatogenic cells fail to adhere to Sertoli cells and are prematurely released from the testis to epididymis. We identified an *N*-glycan structure that plays a key role in germ cell–Sertoli cell adhesion and showed that a specific carbohydrate was required for spermatogenesis.

Spermatogenesis is a complex process by which postmeiotic male germ cells differentiate into mature spermatozoa. At all stages of spermatogenic maturation, germ cells, and Sertoli cells communicate through direct cell-cell contact and paracrine interactions (1). The molecular basis of adhesive interaction between germ cells and Sertoli cells has not been defined (2).

Vertebrate cell surfaces are covered with complex-type *N*-glycans (3). The Golgi  $\alpha$ -mannosidase II (MII) catalyzes the first committed step in the conversion of hybrid to complex-type *N*-glycans (4). In the MII-deficient or *Man2a1* gene knockout mouse, biosynthesis of complex *N*-glycans is not completely impaired (5). This observation suggested the presence of an unknown enzyme that provides an alternate pathway independent from MII. MX is one of the candidates for bypassing MII defect because of its homology with MII (6) and its enzymatic activity (7). However, the biological significance of MX *in vivo* has remained unknown.

The involvement of  $\alpha$ -mannosidases in spermatogenesis has long been suspected (8), because ingestion of locoweed by farm ani-

mals results in male infertility (9). The major “loco-toxin” is swainsonine, an inhibitor of class 2 (glycosylhydrolase family 38)  $\alpha$ -mannosidases (10), which include MII and MX. Class 2 or class 2–related  $\alpha$ -mannosidases (11, 12) expressed on the human sperm cell surface (13), in bull and rat epididymis, and in mouse testis (14–16) are thought to play a role in sperm-egg interaction. These findings suggest a special role for  $\alpha$ -mannosidases and carbohydrates in testis and epididymis in a variety of mammals. Although the expression of MII is fairly widespread in other organs, in the rat testis, MII appears to be restricted to nonspermatogenic Sertoli and Leydig cells (17). The MII-deficient mouse does not show a defect in male reproductive activity (5, 18). These findings suggest a possibility that, in rat and mouse spermatogenic cells, MX plays

a major role in *N*-glycan biosynthesis.

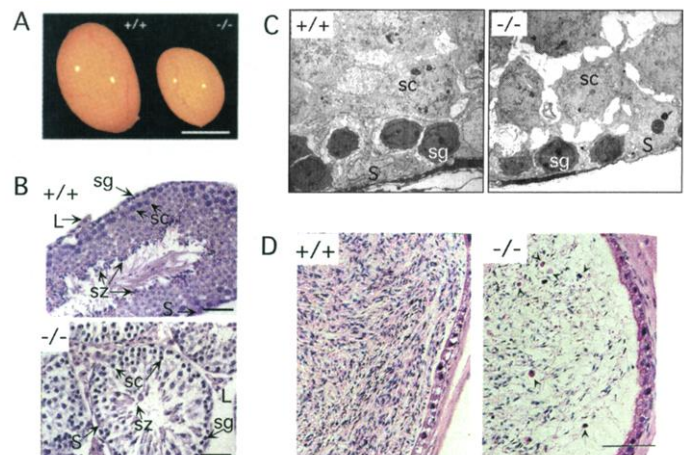
We disrupted *Man2a2*, the gene encoding MX, in embryonic stem (ES) cells by targeted mutation (3). A homologous recombinant ES clone was used to generate chimeric mice and successfully contributed to the germ line. The chimeras were crossed to 129/SVJ mice, and heterozygotes were crossed to produce homozygous mutant offspring (3). The genotyping of pups born from MX<sup>+/+</sup> male and female crosses revealed an unusual ratio of phenotypes: 66 MX<sup>+/+</sup>, 75 MX<sup>+/-</sup>, and 25 MX<sup>-/-</sup>. When MX<sup>+/-</sup> females were crossed with MX<sup>+/+</sup> males, the composition of offspring was 46 MX<sup>+/+</sup> and 46 MX<sup>+/-</sup>. However, when MX<sup>+/+</sup> females were crossed with MX<sup>+/-</sup> males, the offspring included 105 MX<sup>+/+</sup> and 58 MX<sup>+/-</sup>. These observations indicate that either MX-deficient spermatogenic cells are defective, or production of MX-deficient spermatogenic cells is impaired in MX<sup>+/-</sup> males.

Both MX<sup>-/-</sup> males and females were indistinguishable from MX<sup>+/-</sup> and MX<sup>+/+</sup> siblings in growth. No obvious abnormalities in internal organs or behavior were observed in MX<sup>-/-</sup> mice. Whereas MX<sup>-/-</sup> females were fertile, MX<sup>-/-</sup> males were largely infertile, except that some impregnated wild-type females after a prolonged (3-month) mating period and produced small litters of one to three pups.

The testes of MX<sup>-/-</sup> mice were smaller than those of MX<sup>+/+</sup> or MX<sup>+/-</sup> mice (Fig. 1A) (3). Histological analyses of MX<sup>-/-</sup> testes showed that the numbers of spermatogenic cells were significantly reduced (Fig. 1B) (3), whereas nonspermatogenic Sertoli and Leydig cells appeared normal.

Electron microscopy showed that MX<sup>+/+</sup> spermatozoa are closely packed within the seminiferous tubule (Fig. 1C). By contrast, prominent intercellular spaces surrounding

**Fig. 1.** Abnormalities in mouse testis caused by *Man2a2* gene disruption. (A) Testes from an MX<sup>-/-</sup> mouse and an MX<sup>+/+</sup> littermate. Scale bar, 5 mm. (B) Testis sections from MX<sup>+/+</sup> and MX<sup>-/-</sup> mice stained with hematoxylin and eosin. Note that, in MX<sup>-/-</sup> testis, the numbers of late spermatids are significantly reduced compared with those seen in wild-type mice. Scale bars, 50  $\mu$ m. (C) Transmission electron micrographs of MX<sup>+/+</sup> and MX<sup>-/-</sup> mouse testis. (D) Caudal ductus epididymides from MX<sup>+/+</sup> and MX<sup>-/-</sup> mice. Note that epididymis from MX<sup>-/-</sup> mouse contains many immature spermatozoa (shown by arrows) and very few mature spermatozoa. Scale bar, 25  $\mu$ m. L, Leydig cells; sg, spermatogonia; sc, spermatocyte; sz, spermatozoa; S, Sertoli cells.



<sup>1</sup>Glycobiology Program and <sup>2</sup>Stem Cell Program, The Burnham Institute, 10901 North Torrey Pines Road, La Jolla, CA 92037, USA. <sup>3</sup>Biological Science, Graduate School of Science, Hokkaido University, Sapporo, Japan. <sup>4</sup>Department of Obstetrics and Gynecology, Keio University School of Medicine, Tokyo, Japan. <sup>5</sup>Department of Urology, Tohoku University, Sendai, Japan. <sup>6</sup>Departments of Cell & Developmental Biology and Pediatrics, University of North Carolina at Chapel Hill, Chapel Hill, NC 27599, USA. <sup>7</sup>Complex Carbohydrate Research Center, Department of Biochemistry and Molecular Biology, University of Georgia, Athens, GA 30602, USA.

\*To whom correspondence should be addressed. E-mail: michiko@burnham-inst.org

REPORTS

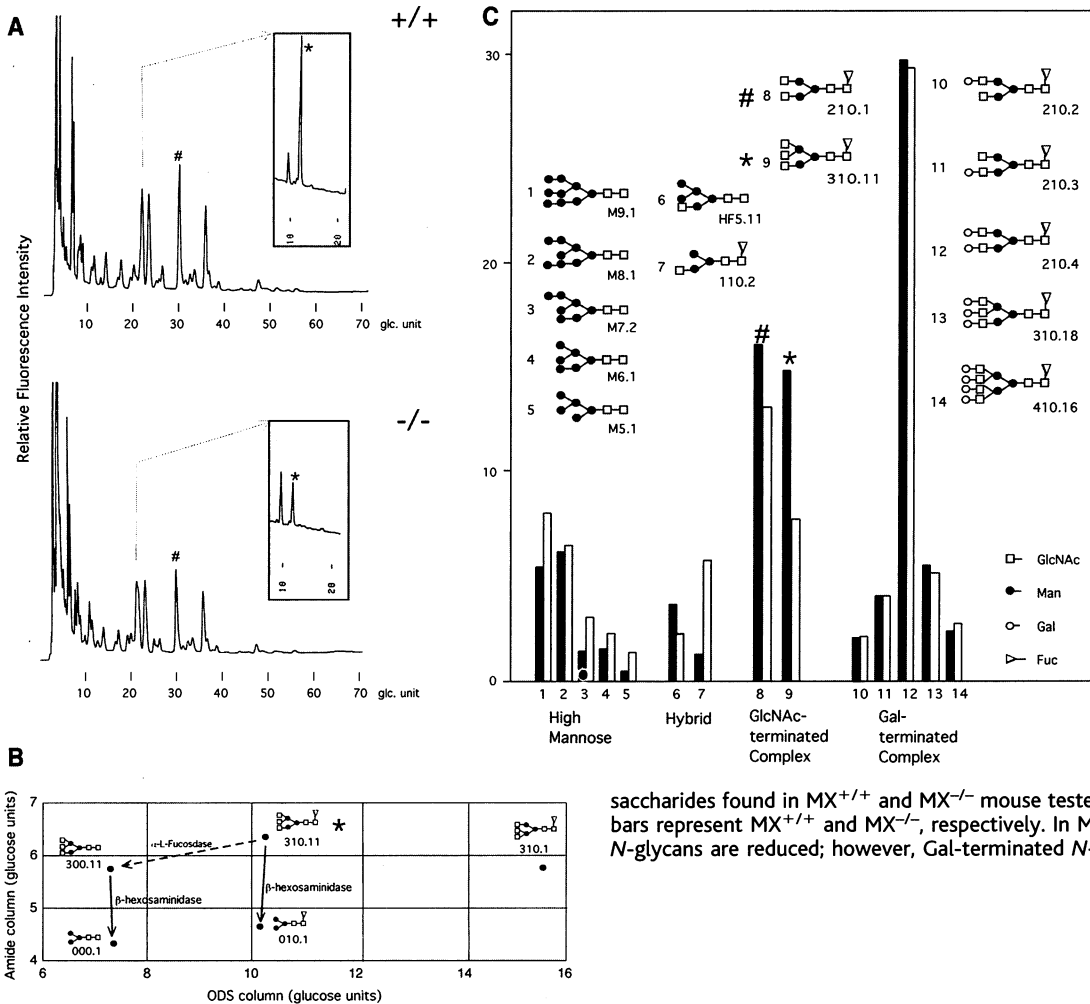
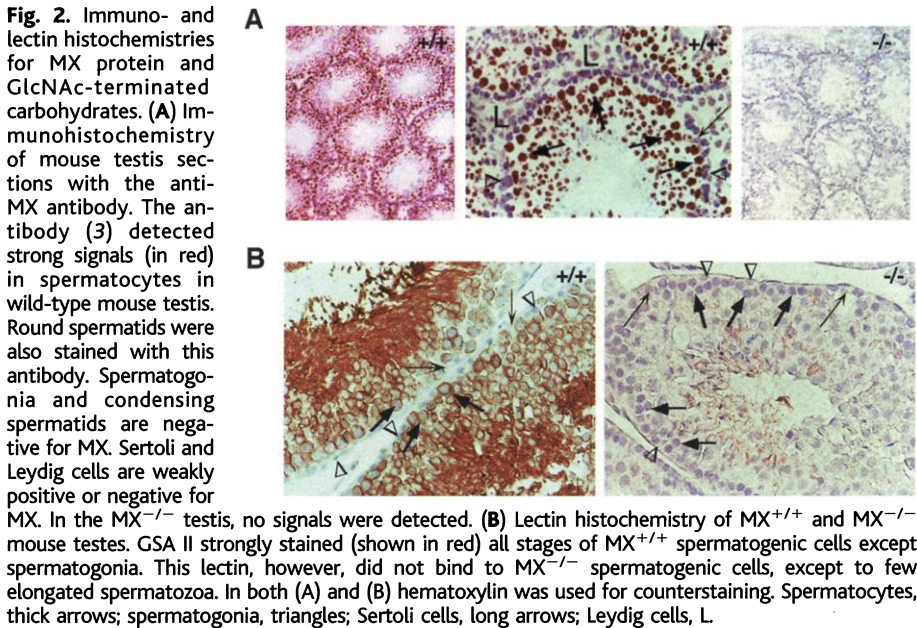
$MX^{-/-}$  spermatocytes suggest a failure of germ-cell adhesion to Sertoli cells within the seminiferous tubules. The caudal ductus epi-

didymis from  $MX^{+/+}$  mouse was packed densely with mature spermatozoa, whereas that from the  $MX^{-/-}$  mouse showed reduced

numbers of spermatozoa (Fig. 1D). Such morphological characteristics of  $MX^{-/-}$  testis and epididymis suggest that spermatogenesis is impaired in  $MX^{-/-}$  mice by the premature release of developing germ cells from the seminiferous epithelium to the epididymis. Thus a failure of spermatogenesis in  $MX^{-/-}$  is not due to an arrest of spermatogenesis, but due to hypospermatogenesis, which is consistent with subfertility of  $MX^{-/-}$  males.

Western blot analysis using the polyclonal (rabbit) antibody against MX detected an expected single band of MX protein at 160 kD in lysates prepared from  $MX^{+/+}$ , but not from  $MX^{-/-}$ , testis (3). Immunohistochemistry with the same antibody revealed strong reactivity in  $MX^{+/+}$  testis in the spermatocytes and round spermatids, but very weak or no reactivities in spermatogonia, condensing spermatids, and nonspermatogenic cells such as Leydig and Sertoli cells (Fig. 2A).

Because MX is an *N*-glycan processing  $\alpha$ -mannosidase (6, 7), a deficiency in MX is expected to affect *N*-glycan biosynthesis. Indeed, histochemistry with *Griffonia simplicifolia* agglutinin (GSA) II, which binds



## REPORTS

to the *N*-acetylglucosamine (GlcNAc) terminal on oligosaccharides, showed marked differences between  $MX^{+/+}$  and  $MX^{-/-}$  testes (Fig. 2B). In  $MX^{+/+}$  testis, spermatogenic cells were strongly stained with this lectin, whereas nonspermatogenic Sertoli and Leydig cells were not stained. In contrast, no staining was detected on  $MX^{-/-}$  germ cells, except in small numbers of condensing spermatids.

Quantitative structural analyses of *N*-glycans from  $MX^{+/+}$  and  $MX^{-/-}$  mouse testis were carried out by a two-dimensional mapping technique (19, 20). These analyses allowed us to determine more than 90% of *N*-glycan structures in  $MX^{+/+}$  and  $MX^{-/-}$

testes (Fig. 3).  $MX^{+/+}$  testes ( $n = 4$ ) contained complex-type *N*-glycans with GlcNAc termini, a result consistent with strong GSA II lectin staining (Fig. 2B) (3). Thus, mouse testes contain a rare oligosaccharide 210.1 (marked by # in Fig. 3, A and C) and a previously unknown oligosaccharide 310.11 (Fig. 3B, marked by \* in Fig. 3, A to C).

In  $MX^{-/-}$  testes ( $n = 3$ ), the levels of GlcNAc-terminated oligosaccharides are reduced (Fig. 3C). These findings suggest that GlcNAc-terminated *N*-glycans are produced in an *MX*-dependent manner in spermatogenic cells. In contrast, the *Man2a2* null mutation did not affect the levels of Gal-terminated *N*-glycans (Fig. 3C) (3).

As electron micrographs suggested a failure of spermatogenic cells to adhere to Sertoli cells in  $MX^{-/-}$  testis (Fig. 1C), we examined adhesion of spermatogenic cells to Sertoli cells using an *in vitro* assay (21–23). We found that the apparent failure in germ cell–Sertoli cell adhesion seen in  $MX^{-/-}$  mice is due to a defect in spermatogenic cells, not in Sertoli cells (Fig. 4, A and B). As reported previously (21), fixed wild-type spermatogenic cells adhered to Sertoli cells (Fig. 4, A and B), suggesting that a carbohydrate expressed on the surface of spermatogenic cells is responsible for germ cell adhesion to Sertoli cells.

To test directly an involvement of *N*-glycans in germ cell–Sertoli cell adhesion, we prepared mouse testis *N*-glycans and tested their effects on germ cell–Sertoli cell adhesion. Glycopeptides from  $MX^{+/+}$  testes strongly inhibited adhesion in a dose-dependent manner, whereas those from  $MX^{-/-}$  testes exhibited minimal activity (Fig. 4C). None of the glycopeptides prepared from ovalbumin,  $\alpha_1$ -acid glycoprotein, and fibrinogen showed inhibitory activity at 200  $\mu$ g (as hexose)/ml (24).

To determine which *N*-glycan structure is involved in the germ cells' adhesion to Sertoli cells, each purified oligosaccharide was tested for potential inhibitory activity (Fig. 4D). The result demonstrated that 310.11 has a strong inhibitory activity, whereas other *N*-glycans tested did not show such activity. This finding indicates that 310.11, a GlcNAc-terminated tri-antennary and fucosylated *N*-glycan structure newly identified in this study, plays a key role in germ cell–Sertoli cell adhesion. Given that 50% reduction of 310.11 but almost no binding of  $MX^{-/-}$  spermatogenic cells with GSA II and Sertoli cells, a presumptive 310.11 receptor on Sertoli cells may have binding properties similar to GSA II, which appears to be sensitive to threshold and/or multivalency of 310.11.

Cell-surface glycans are often viewed as modulators that prevent access of ligand to a membrane receptor (25–27). Also, the glycans themselves serve as specific ligands (28–30). In this study, we have identified carbohydrates acting in a biologically critical event. Our study provides a clue for further defining the mechanisms underlying germ cell–Sertoli cell interactions in mammals. Availability of the  $MX^{-/-}$  mutant mice will facilitate further analysis of spermatogenesis in the mouse and may further our understanding of male infertility in humans.

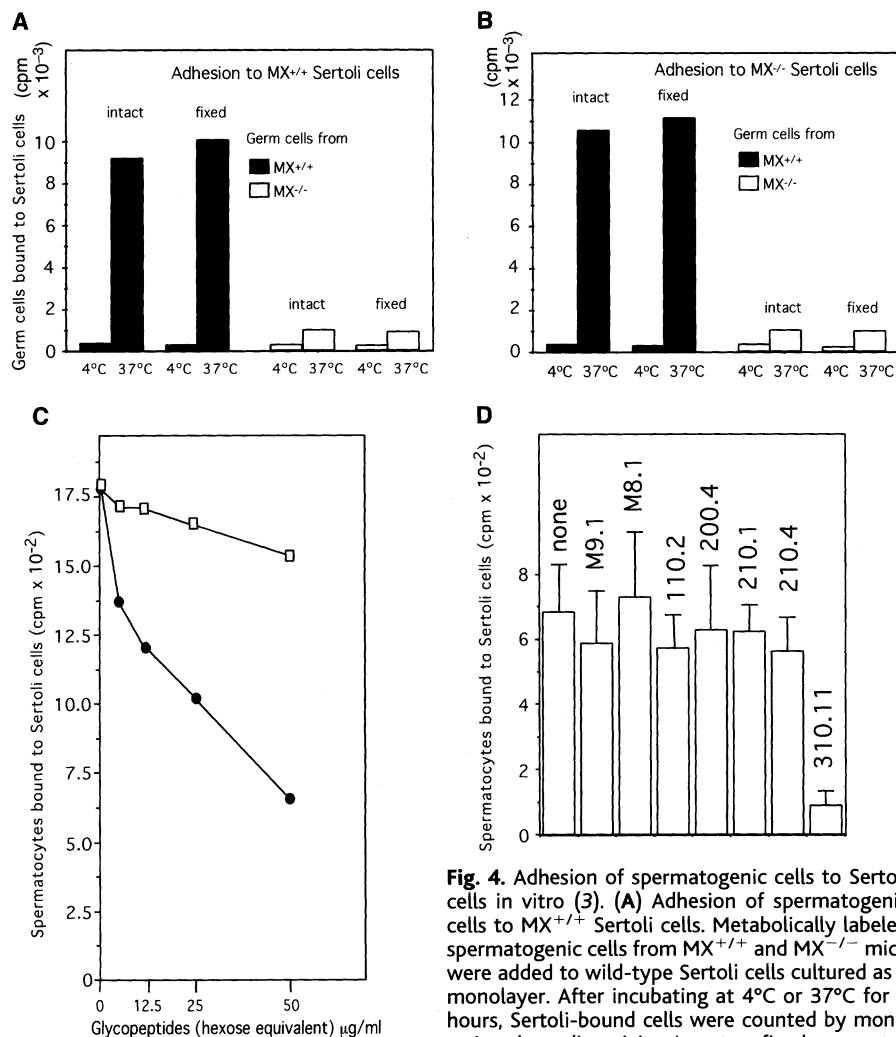


**Fig. 4.** Adhesion of spermatogenic cells to Sertoli cells *in vitro* (3). (A) Adhesion of spermatogenic cells to  $MX^{+/+}$  Sertoli cells. Metabolically labeled spermatogenic cells from  $MX^{+/+}$  and  $MX^{-/-}$  mice were added to wild-type Sertoli cells cultured as a monolayer. After incubating at 4°C or 37°C for 4 hours, Sertoli-bound cells were counted by monitoring the radioactivity. Intact or fixed spermatogenic cells were tested. (B) Adhesion of spermatogenic cells to  $MX^{-/-}$  Sertoli cells. The experiment was conducted in the same manner as in (A), except that  $MX^{-/-}$  Sertoli cells were used. (C) Inhibition of germ cell–Sertoli cell adhesion by glycopeptides prepared from  $MX^{+/+}$  or  $MX^{-/-}$  mouse testes. Intact and radiolabeled  $MX^{+/+}$  spermatogenic cells were added to Sertoli cells in the presence or absence of glycopeptides from  $MX^{+/+}$  (filled circles) or  $MX^{-/-}$  (open squares) mouse testes, and incubated at 37°C for 4 hours. (D) Inhibition of germ cell–Sertoli cell adhesion with purified testis *N*-glycan oligosaccharides.  $MX^{+/+}$  spermatogenic cells were added to Sertoli cells in the presence (columns 2 to 8) or absence (column 1) of 2  $\mu$ M each PA-oligosaccharide. Oligosaccharide 200.4 is 210.4 minus fucose. In (A), (B), and (C), each value represents the average of duplicate measurements. In (D) each value represents the average of triplicate measurements.

genic cells to  $MX^{-/-}$  Sertoli cells. The experiment was conducted in the same manner as in (A), except that  $MX^{-/-}$  Sertoli cells were used. (C) Inhibition of germ cell–Sertoli cell adhesion by glycopeptides prepared from  $MX^{+/+}$  or  $MX^{-/-}$  mouse testes. Intact and radiolabeled  $MX^{+/+}$  spermatogenic cells were added to Sertoli cells in the presence or absence of glycopeptides from  $MX^{+/+}$  (filled circles) or  $MX^{-/-}$  (open squares) mouse testes, and incubated at 37°C for 4 hours. (D) Inhibition of germ cell–Sertoli cell adhesion with purified testis *N*-glycan oligosaccharides.  $MX^{+/+}$  spermatogenic cells were added to Sertoli cells in the presence (columns 2 to 8) or absence (column 1) of 2  $\mu$ M each PA-oligosaccharide. Oligosaccharide 200.4 is 210.4 minus fucose. In (A), (B), and (C), each value represents the average of duplicate measurements. In (D) each value represents the average of triplicate measurements.

### References and Notes

- J. B. Kerr, *Microsc. Res. Tech.* **32**, 364 (1995).
- B. Jegou, *Int. Rev. Cytol.* **147**, 25 (1993).
- Supplementary material is available on Science Online at [www.sciencemag.org/content/full/295/5552/124/DC1](http://www.sciencemag.org/content/full/295/5552/124/DC1).
- R. Kornfeld, S. Kornfeld, *Annu. Rev. Biochem.* **54**, 631–664 (1985).
- D. Chui *et al.*, *Cell* **90**, 157 (1997).

6. M. Misago *et al.*, *Proc. Natl. Acad. Sci. U.S.A.* **92**, 11766 (1995).
7. M. Oh-eda *et al.*, *Eur. J. Biochem.* **268**, 1280 (2001).
8. D. R. P. Tulsiani, H. Yoshida-Komiya, Y. Araki, *Biol. Reprod.* **57**, 487 (1997).
9. K. E. Panter *et al.*, *J. Nat. Toxins* **8**, 53 (1999).
10. D. R. P. Tulsiani, T. M. Harris, O. Touster, *J. Biol. Chem.* **257**, 7936 (1982).
11. B. Henrissat, *Biochem. Soc. Trans.* **26**, 153 (1998).
12. K. W. Moremen, in *A Comprehensive Handbook*, B. Ernst, G. Hart, P. Sinay, Eds., (Wiley, New York, 2000), p. 81.
13. D. R. P. Tulsiani, M. D. Skudlarek, M.-C. Orgebin-Crist, *Biol. Reprod.* **42**, 843 (1990).
14. S. Hiramoto *et al.* *Biochem. Biophys. Res. Comm.* **241**, 439 (1997).
15. M. D. Skudlark, M.-C. Orgebin-Crist, D. R. P. Tulsiani, *Biochem. J.* **277**, 213 (1991).
16. D. R. P. Tulsiani, M. D. Skudlarek, M.-C. Orgebin-Crist, *J. Cell. Biol.* **109**, 1257 (1989).
17. S. A. Igdoura *et al.* *Eur. J. Cell Biol.* **78**, 441 (1999).
18. D. Chui *et al.*, *Proc. Natl. Acad. Sci. U.S.A.* **98**, 1142 (2001).
19. N. Takahashi, N. Tomiya, in *Handbook of Endoglycosidases and Glycoamidases*, N. Takahashi, T. Muramatsu, Eds. (CRC Press, Boca Raton, FL, 1992), pp. 199–332.
20. H. Nakagawa *et al.*, *Anal. Biochem.* **226**, 138 (1995).
21. R. M. DePhilip, D. G. Danahey, *Biol. Reprod.* **37**, 1271 (1987).
22. S. Kohno, E. Ziparo, L. F. Marek, K. S. Tung, *J. Reprod. Immunol.* **5**, 339 (1983).
23. Although the reported adhesion assays were performed at 32°C, we performed the assay at 37°C, because small numbers of MX<sup>-/-</sup> spermatogenic cells adhered to Sertoli cells at 32°C presumably by an additional mechanism independent from MX defect.
24. T. O. Akama, M. N. Fukuda, unpublished observations.
25. D. J. Moloney *et al.*, *Nature* **406**, 369 (2000).
26. M. Demetriou, M. Granovsky, S. Quaggin, S. J. W. Dennis, *Nature* **409**, 733 (2001).
27. S. Tsuboi, M. Fukuda, *EMBO J.* **16**, 6364 (1997).
28. P. Maly *et al.*, *Cell* **86**, 643 (1996).
29. I. Stamenkovic, D. Sgroi, A. Aruffo, *Cell* **68**, 1003A (1992).
30. L. G. Baum *et al.*, *J. Exp. Med.* **181**, 877 (1995).
31. Available at [www.gak.co.jp/FCCA](http://www.gak.co.jp/FCCA).
32. The authors thank E. Ruoslahti, E. Adamson, Y. Yamaguchi, M. Fukuda, and E. Lamar; for critical readings of the manuscript; M. Dym and N. B. Hecht for suggestions; R. DePhilip for instruction for germ cell–Sertoli cell adhesion assay; M. Oh-eda, M. Misago, R. Aoki, S. Saburi, and J. Zhang for discussions; and A. Pai for technical assistance. The present study was supported by NIH grants CA71932 (to M.N.F.), GM47533 and RR05351 (to K.W.M.), CA 42595 and HD05863 (to J.L.M.), and BCRP 4KB-0106 (to S.N.).

21 August 2001; accepted 1 November 2001

## Combined Functional Genomic Maps of the *C. elegans* DNA Damage Response

Simon J. Boulton,<sup>1,2</sup> Anton Gartner,<sup>3</sup> Jérôme Reboul,<sup>1</sup> Philippe Vaglio,<sup>1</sup> Nick Dyson,<sup>2</sup> David E. Hill,<sup>1</sup> Marc Vidal<sup>1\*</sup>

Many human cancers originate from defects in the DNA damage response (DDR). Although much is known about this process, it is likely that additional DDR genes remain to be discovered. To identify such genes, we used a strategy that combines protein-protein interaction mapping and large-scale phenotypic analysis in *Caenorhabditis elegans*. Together, these approaches identified 12 worm DDR orthologs and 11 novel DDR genes. One of these is the putative ortholog of hBCL3, a gene frequently altered in chronic lymphocytic leukemia. Thus, the combination of functional genomic mapping approaches in model organisms may facilitate the identification and characterization of genes involved in cancer and, perhaps, other human diseases.

Inherited cancer predisposition syndromes such as Li-Fraumeni syndrome, xeroderma pigmentosum, and hereditary nonpolyposis colon cancer result from defects in DNA repair or DNA damage checkpoint pathways (collectively referred to as the DDR) (1). In wild-type cells, checkpoint pathways induce a transient cell-cycle arrest in response to DNA damage, thus providing the necessary time for DNA repair to occur, and a variety of DNA repair pathways correct the various types of DNA lesions (2). Alternatively, in metazoan organisms, checkpoint pathways can also induce apoptosis, thereby eliminating compromised cells (3). *Caenorhabditis elegans* is the simplest metazoan model organism that can be used to study the DDR (4, 5). After DNA damage, checkpoint pathways induce cell-cycle arrest or apoptosis of

mitotic or pachytene cells of the adult germ line, respectively. These two cell types are located in spatially distinct regions.

To identify novel *C. elegans* DDR genes, we used a combination of functional genomic mapping approaches. High-throughput (HT) methods such as transcription profiling, protein interaction mapping, and large-scale phenotypic analysis have been applied individually to worm biology with considerable success (6, 7). Consequently, hypotheses of function are now available for hundreds of previously uncharacterized genes. Although no single HT method can unequivocally define gene function, combining the data obtained from any of these complementary approaches is likely to provide greater functional insight (7). Here we have chosen to combine protein-protein interaction mapping and HT phenotypic analysis for the following three reasons. Because the function of most known DDR proteins is based on their ability to mediate protein-protein interactions, putative *C. elegans* DDR orthologs were used to generate a DDR protein interaction map. To demonstrate biological relevance, defects in the DDR were then analyzed systematically for each of the corre-

sponding genes after HT RNA-mediated interference (RNAi). Lastly, in addition to potentially identifying novel DDR genes, combining these two approaches has the advantage of providing potential insights into how the corresponding proteins function, on the basis of the identity of their interacting partners.

To date, only three genes (*mrt-2*, *rad-51*, and *mre-11*) have been experimentally implicated in the *C. elegans* DDR (4, 5, 8). To identify potential worm DDR orthologs, we used known DDR proteins, including those implicated in nucleotide excision repair (NER), mismatch repair (MR), base excision repair (BER), nonhomologous end joining (NHEJ), homologous recombination (HR), and checkpoint pathways, as to query the *C. elegans* predicted proteome by BLAST [see legend to Web table 1 (9)]. A total of 75 putative *C. elegans* DDR orthologous open reading frames (dORFs) were identified and cloned using the Gateway recombinational cloning system (10) (Web table 1). The dORFs were then transferred to two-hybrid destination vectors to express either DNA binding domain (DB) fusions (DB-dORFs) or activation domain (AD) fusions (AD-dORFs) for protein-protein interaction analysis (11).

Conserved interactions, or interologs (12), were anticipated among worm DDR proteins on the basis of interactions reported between their potential orthologs in other organisms. To identify such DDR interologs, we first tested all possible pairwise combinations between the 75 DB-dORFs and AD-dORFs in a matrix setting. Among 33 putative interologs, 17 scored positive in the two-hybrid matrix (Table 1 and Web fig. 1). This represents a 51% success rate in detecting predicted protein interactions using this yeast two-hybrid system, which is in the same range as has been described previously for other protein interaction mapping projects (13). If one assumes that conservation of interaction between two putative orthologs is a reasonable indication of functional conservation, our search for interologs would suggest that at least 30 predicted worm DDR proteins are bona fide orthologs.

<sup>1</sup>Dana-Farber Cancer Institute and Department of Genetics, Harvard Medical School, Boston, MA 02115, USA. <sup>2</sup>Massachusetts General Hospital Cancer Center, Charlestown, MA 02129, USA. <sup>3</sup>Max Planck Institute for Biochemistry, D 82152 Martinsried, Germany.

\*To whom correspondence should be addressed. E-mail: [marc\\_vidal@dfci.harvard.edu](mailto:marc_vidal@dfci.harvard.edu)